Infection, Genetics and Evolution 96 (2021) 105131

Contents lists available at ScienceDirect

Infection, Genetics and Evolution

journal homepage: www.elsevier.com/locate/meegid

Pseudomonas putida group species as reservoirs of mobilizable Tn*402*-like class 1 integrons carrying *bla*$_{VIM-2}$ metallo-β-lactamase genes

Marco A. Brovedan [a], Patricia M. Marchiaro [a], María S. Díaz [a], Diego Faccone [b], Alejandra Corso [b], Fernando Pasteran [b], Alejandro M. Viale [a,*], Adriana S. Limansky [a,*]

[a] *Instituto de Biología Molecular y Celular de Rosario (IBR, CONICET), Facultad de Ciencias Bioquímicas y Farmacéuticas, Universidad Nacional de Rosario, Rosario, Argentina*

[b] *Servicio Antimicrobianos, Departamento de Bacteriología, Instituto Nacional de Enfermedades Infecciosas-ANLIS "Dr. Carlos G. Malbrán", Ciudad Autónoma de Buenos Aires, Argentina*

ARTICLE INFO

Keywords:
Pseudomonas putida group
Carbapenem resistance plasmids
Tn*402*-like class 1 integrons
VIM-2 metallo-β-lactamase reservoirs
Mobile genetic elements
Tn*21*

ABSTRACT

The *Pseudomonas putida* group (*P. putida* G) is composed of at least 21 species associated with a wide range of environments, including the clinical setting. Here, we characterized 13 carbapenem-resistant *P. putida* G clinical isolates bearing class 1 integrons/transposons (class 1 In/Tn) carrying *bla*$_{VIM-2}$ metallo-β-lactamase gene cassettes obtained from hospitals of Argentina. Multilocus sequencing (MLSA) and phylogenetic analyses based on 16S rDNA, *gyrB* and *rpoD* sequences distinguished 7 species among them. *bla*$_{VIM-2}$ was found in three different cassette arrays: In41 (*bla*$_{VIM-2}$-*aacA4*), In899 (only *bla*$_{VIM-2}$), and In528 (*dfrB1*-*aacA4*-*bla*$_{VIM-2}$). In41 and In899 were associated with complete *tniABQC* transposition modules and IRi/IRt boundaries characteristic of the Tn*5053*/Tn*402* transposons, which were designated Tn*6335* and Tn*6336*, respectively. The class 1 In/Tn element carrying In528, however, exhibited a defective *tni* module bearing only the *tniC* (transposase) gene, associated with a complete IS*6100* bounded with two oppositely-oriented IRt end regions. In some *P. putida* G isolates including *P. asiatica*, *P. juntendi*, *P. putida* G/II, and *P. putida* G/V, Tn*6335*/Tn*6336* were carried by pLD209-type conjugative plasmids capable of self-mobilization to *P. aeruginosa* or *Escherichia coli*. In other isolates of *P. asiatica*, *P. putida* G/II, and *P. monteiliieilii*, however, these *bla*$_{VIM-2}$-containing class 1 In/Tn elements were found inserted into the *res* regions preceding the *tnpR* (resolvase) gene of particular Tn*21* subgroup members of Tn*3* transposons. The overall results reinforce the notion of *P. putida* G members as *bla*$_{VIM-2}$ reservoirs, and shed light on the mechanisms of dissemination of carbapenem resistance genes to other pathogenic bacteria in the clinical setting.

1. Introduction

The bacterial organisms composing the *Pseudomonas* genus are ubiquitous in nature, and thrive in very different ecological niches including soils, water, sediments, air, and human environments (Mulet et al., 2010, 2013; Peix et al., 2018; Tohya et al., 2019a, 2019b). *Pseudomonas* members are endowed with a wide metabolic versatility and a broad adaptive potential to challenging environmental conditions. The genus includes pathogenic lineages of species such as *P. aeruginosa*, which have evolved resistance to most classes of antimicrobial agents of clinical use (multidrug resistance, MDR), including last-resource therapeutic options such as the carbapenems (Yoon and Jeong, 2021). Horizontal gene transfer of resistance genes from other bacteria inhabiting the same ecological niches has certainly contributed to the ability of *P. aeruginosa* to evolve MDR (Yoon and Jeong, 2021).

Different phenotypic and chemotaxonomic features have been extensively used in *Pseudomonas* classification, but much more reliable approaches are represented by genomic-based procedures (Mulet et al., 2010, 2013; Peix et al., 2018; Tohya et al., 2019a, 2019b). In this context, multilocus sequence analysis (MLSA) approaches using selected core genes such as 16S rDNA, *gyrB*, *rpoB*, and *rpoD* genes have been widely employed for a more precise definition of the "species" boundaries among *Pseudomonas* isolates (Mulet et al., 2010, 2013; Peix et al., 2018; Tohya et al., 2019a, 2019b). These procedures have allowed to differentiate (at least) 21 species within the so-called *P. putida* group (*P. putida* G). Among them *P. putida*, *P. monteilii*, *P. fulva*, *P. mosselii*, and

* Corresponding authors.
E-mail addresses: viale@ibr-conicet.gov.ar (A.M. Viale), limansky@ibr-conicet.gov.ar (A.S. Limansky).

https://doi.org/10.1016/j.meegid.2021.105131
Received 30 June 2021; Received in revised form 15 October 2021; Accepted 2 November 2021
Available online 6 November 2021

newly assigned *P. putida* G species such as *P. asiatica* (heterotypic synonym, *P. shirazica*) and *P. juntendi* have been more recently associated with human infections (Marchiaro et al., 2014; Seok et al., 2010; Tohya et al., 2019a, 2019b; Treviño et al., 2010; Yamamoto et al., 2018). Although most *P. putida* G clinical isolates exhibited in the past general susceptibility to most clinically-employed antimicrobials, an emerging resistance to carbapenems has been reported more recently among them. This resistance has been accompanied by the detection of metallo-β-lactamases (MβLs) of the VIM, IMP, DIM, or NDM families, suggesting that *P. putida* G members represent active reservoirs of the corresponding genes (Almuzara et al., 2007; Bogaerts et al., 2011; Juan et al., 2010; Lee et al., 2002; Loucif et al., 2017; Marchiaro et al., 2010; Peter et al., 2017; Santos et al., 2010; Scotta et al., 2011; Walsh et al., 2005).

The bla_{VIM-2} MβL gene is the most frequently found among the genomes of *P. aeruginosa* clinical isolates obtained worldwide, and is commonly linked to high-risk clones exhibiting MDR phenotypes (Botelho et al., 2018b; Papagiannitsis et al., 2017, 2020; Yoon and Jeong, 2021). bla_{VIM-2} is generally found in these isolates as forming part of the cassette repertoire of class 1 integrons/transposons (class 1 In/Tn) located in the chromosome or in plasmids (Botelho et al., 2018a, 2018b; Jeong et al., 2009; Lee et al., 2002; Molina-Mora et al., 2021; Papagiannitsis et al., 2017, 2020; Perez et al., 2014; Quinones-Falconi et al., 2010; Van der Zee et al., 2018; Walsh et al., 2005; Yoon and Jeong, 2021). Although class 1 In/T (also designated as Tn*402*-like elements) show both remarkable gene context complexity and variety in the associated cassettes, their common structural elements include the characteristic inverted repeats IRi and IRt of the Tn*5053*/Tn*402* family of transposons along with constitutive sequences between them, such as the 5′-conserved segment (5′-CS) adjacent to the IRi encompassing the integrase gene (*intI1*), the *attI* site into which the cassettes are incorporated, and the Pc, as well as other downstream promoters (such as P2) directing expression of the cassette genes (Betteridge et al., 2011; Botelho et al., 2018b; Gillings, 2014; Kholodii et al., 1995; Papagiannitsis et al., 2009, 2020; Partridge et al., 2001, 2018; Yoon and Jeong, 2021). To the right of the last cassette, most class 1 In/Tn found in *P. aeruginosa* clinical isolates and in other pathogens contain a region known as the 3′-conserved segment (3′-CS), which includes *qacEΔ1,* derived from the *qacE* cassette (encoding resistance to quaternary ammonium compounds) and *sul1* conferring resistance to sulfonamide, and two other genes of poorly defined function. In other class 1 In/Tn the 3′-CS (or parts of it) is adjoined by a number of insertion sequences (IS), from which IS*6100* flanked by inverted repeats of the IRt end represents a commonly found structural element (Partridge et al., 2001, 2018). There is a general consensus that this variety of Tn*402*-like backbone structures derive from a common ancestor of the Tn*5053*/Tn*402* transposon family already carrying the integron, but containing in place of the 3′-CS a complete *tniABQC* module composed of *tniA*, *tniB*, and *tniQ* genes involved in transposition, and a resolvase *tniC* (or *tniR*) gene involved in the resolution of the cointegrates formed as transpositional intermediates (Betteridge et al., 2011; Gillings, 2014; Kholodii et al., 1995; Nicolas et al., 2015; Partridge et al., 2001, 2018; Rådström et al., 1994; Yoon and Jeong, 2021). Expectedly from the above observations, many class 1 In/Tn found in clinical strains represent incomplete transposons, but evidence exists that some assemblages can be moved if the appropriate functions are provided in trans (Partridge et al., 2001, 2018). Moreover, the demonstrated ability of the Tn*402* transposition system to target *res* sites located on Tn*21* subgroup members of the Tn*3* transposon family, or the equivalent *par* sites of some plasmids, has led to the spread of class 1 In/Tn to a range of different mobile genetic elements (MGE) including transposons, plasmids, integrative conjugative elements (ICEs) and genomic islands (GIs) (Botelho et al., 2018a, 2018b; Gillings, 2014; Jeong et al., 2009; Lee et al., 2002; Molina-Mora et al., 2021; Minakhina et al., 1999; Nicolas et al., 2015; Papagiannitsis et al., 2017, 2020; Partridge et al., 2001, 2018; Perez et al., 2014; Van der Zee et al., 2018; Yoon and Jeong, 2021). The overall results additionally emphasize how different MGEs can lead to novel rearrangements, collectively spreading resistance genes with the subsequent difficulties in therapeutic management.

The observations above summarize the large mass of information collected on the genetic contexts of class 1 In/Tn carrying bla_{VIM-2} in clinical *P. aeruginosa* isolates, but fewer data exist on other members of the *Pseudomonas* genus considered as reservoirs of MβL genes such as *P. putida* G members (Almuzara et al., 2007; Bogaerts et al., 2011; Juan et al., 2010; Lee et al., 2002; Loucif et al., 2017; Marchiaro et al., 2010; Peter et al., 2017; Santos et al., 2010; Scotta et al., 2011; Walsh et al., 2005). The reconstruction of the genomic context of bla_{VIM-2}-containing Tn*402*-like elements in these reservoirs conducted in this work may thus provide insights not only into their evolution in association with human activities, but also identify possible ways to mitigate the spreading of these genes to pathogenic bacteria sharing the clinical niche.

2. Materials and methods

2.1. Bacterial isolates and antimicrobial susceptibility testing

Thirteen carbapenem-resistant clinical isolates initially identified as *P. putida* by the Vitek 2C System (bioMérieux, Marcy l'Etoile, France) were selected for this study (Table 1) from a collection of clinical *P. putida* isolates. These isolates were collected from inpatients of different hospitals of Buenos Aires (B1-B3) or Rosario (R1-R5), Argentina, during the period 2006–2014 (Table S1). The susceptibilities of these isolates to different antimicrobials including imipenem, meropenem, ceftazidime, cefepime, piperacillin-tazobactam, gentamicin, amikacin, and ciprofloxacin, Table S1) were evaluated using the Vitek 2C System (bioMérieux, Marcy l'Etoile, France). The interpretation of the MIC values shown in Table S1 was based on CLSI breakpoints recommendations (Clinical and Laboratory Standards Institute (CLSI), 2019).

2.2. Assignment of P. putida G clinical isolates to the species level

The assignment of the clinical isolates to the species level was based on multilocus sequencing analysis (MLSA) and sequence comparisons following described procedures (Mulet et al., 2010, 2013). This approach is based on the percentage of nucleotide sequence identity between alignments of the concatenated sequences here employed (2,276 bp in total), corresponding to partial regions of the 16S rDNA (930 bp), *gyrB* (669 bp) and *rpoD* (677 bp) genes. Also, a 97.0% identity as the threshold value that separates species within the *P. putida* group was used (Mulet et al., 2013). Genomic DNA was purified from the different clinical isolates using Wizard Genomic DNA Purification Kit (Promega, Madison, WI), and used as template for PCR reactions aimed to amplify the desired fragments of the 16S rDNA, *gyrB* and *rpoD* genes used for concatenate constructions (Table S2). The corresponding partial sequences from type strains including 21 species of *P. putida* G, *P. aeruginosa* ATCC 10145, and *P. oryzihabitans* ATCC 43272, as well as those corresponding to representative members of 6 *P. putida* G newly proposed species (Mulet et al., 2013) were retrieved from the sequence data deposited on the NCBI database (Table S3). The alignments of concatenated genes were done using ClustalW with default parameters (https://www.genome.jp/tools-bin/clustalw).

A Maximum-Likelihood (ML) phylogenetic tree was also constructed from the above alignments using MEGA7.0 (Kumar et al., 2016). To determine the best-fit nucleotide substitution model, the tool included in MEGA7.0 was employed resulting in the use of the GTR + G + I substitution model, taking into account the Akaike information criterion (AIC). Only branches supported by bootstrap values higher than 60% (1,000 replicates) were included in the tree.

The clonal relatedness among isolates assigned to a same *P. putida* G species was evaluated by a random amplification PCR assay employing degenerate oligonucleotides (DO-PCR) (Limansky and Viale, 2002).

Table 1
Characterization of *Pseudomonas putida* group clinical isolates used in this study.

Isolate[a]	Percentage of core genes concatenate nucleotide similarity between isolates and the closest reference species (between brackets)[b]	Percentage of core genes concatenate nucleotide similarity between isolates and the closest newly proposed species (between brackets)[c]	Species assignment[d]	Clone[e]	Identified Tn*5053*/Tn*402* family transposon[f]	Detection of conjugative plasmids harboring bla_{VIM-2}[g]
BA9115	99.51 (*P. putida*)		*P. putida*	Pp_B	Tn*6336*	–
BA7908	99.56 (*P. putida*)		*P. putida*	Pp_A	Tn*6335*	–
BA9713	98.76 (*P. monteilii*)		*P. monteilii*	Pm_B	Tn*6335*	–
HB157	98.59 (*P. monteilii*)		*P. monteilii*	Pm_A	Tn*402*Δ(*tniABQ*)	–
BA7816	98.72 (*P. asiatica*)	97.88 (*P. putida* G/IV)	*P. asiatica*	Pa_B	Tn*6336*	+
LD209	99.91 (*P. asiatica*)	98.14 (*P. putida* G/IV)	*P. asiatica*	Pa_A	Tn*6335*	+
HP613	99.91 (*P. asiatica*)	98.14 (*P. putida* G/IV)	*P. asiatica*	Pa_A	Tn*6335*	–
HB313	99.91 (*P. asiatica*)	98.14 (*P. putida* G/IV)	*P. asiatica*	Pa_A	Tn*6335*	+
HP813	96.35 (*P. monteilii*)	98.90 (*P. putida* G/I)	*P. putida* G/I	–	Tn*6335*	–
HE1012	96.22 (*P. monteilii*)	99.25 (*P. putida* G/II)	*P. putida* G/II	$PpGII_B$	Tn*6335*	+
LA1008	96.92 (*P. monteilii*)	99.86 (*P. putida* G/II)	*P. putida* G/II	$PpGII_A$	Tn*6335*	–
BA9605	92.92 (*P. plecoglossicida*)	97.71 (*P. putida* G/V)	*P. putida* G/V	–	Tn*6335*	+
LA111	99.25 (*P. juntendi*)		*P. juntendi*	–	Tn*6335*	+

[a] All *P. putida* G clinical isolates were obtained from Hospitals of Buenos Aires City (BA) (a collection of the Malbrán Institute, Buenos Aires), or Rosario City (HB, LD, HP, LA), Argentina. Further details on their sources, year of isolation, and antimicrobial resistance profiles are given in Table S1.

[b] Percentages of nucleotide similarity between concatenates of 16S rDNA, *gyrB* and *rpoD* selected gene fragments of the analyzed isolates and the equivalent sequences of the closest assigned reference (type) *P. putida* G strain. The reference strains and the accession numbers of the corresponding core gene sequences are shown in Table S3.

[c] Percentages of nucleotide similarity between concatenates of 16S rDNA, *gyrB* and *rpoD* selected gene fragments of the analyzed isolates and the equivalent sequences of newly proposed *P. putida* species (Mulet et al., 2013; G/I, G/II, G/IV, G/V).

[d] The assignment of a given isolate at the species level was based on the highest percentage of nucleotide similarity found between the corresponding core gene concatenates shown above.

[e] Clonal differentiation between isolates assigned to a given species as defined above as determined by a random amplification PCR assay (see. Fig. S1). The different profiles found in each case are distinguished using subscript capital letters which were arbitrarily chosen.

[f] Following Tn Number Registry (http://transposon.lstmed.ac.uk/).

[g] The presence of plasmids carrying bla_{VIM-2} was tested by conjugation assays. In addition, the self-transferability of the plasmids was tested. When no transconjugants were obtained, transformation assays were done. +: transconjugants detected; −: neither transconjugants nor transformants detected.

2.3. Detection of MβL by phenotypic and molecular methods

MβL activity in all isolates included in this study was revealed by two screening methods including EDTA-imipenem microbiological assay (EIM) and EDTA disk synergy test (EDS) previously reported (Marchiaro et al., 2005). The presence of bla_{VIM}-, bla_{IMP}-, bla_{SPM-1}- or bla_{NDM}-like genes was evaluated by PCR using specific primers (Table S2).

2.4. Genetic context of bla_{VIM-2} genes in the P. putida G isolates analyzed

The association of bla_{VIM-2} genes with class 1 In/Tn was analyzed by PCR using conventional primer pairs (Marchiaro et al., 2010; see Table S2). Amplification bands obtained by the use of the primer pair 5'-CS (forward) and TniC-R2 (reverse) (Table S2) were subjected to sequencing analysis (Marchiaro et al., 2010). The complete structures of the Tn*402*-like elements were further obtained by PCR-overlapping assays using genomic DNA from each isolate and appropriate pairs of primers (Table S2), followed by sequencing and database searching analyses as described in detail previously (Marchiaro et al., 2010). The left boundary sequences of the Tn*402*-like transposons from the IRi to the bla_{VIM-2} gene were determined by PCR using the primer combination IRHP/VIM-R, and the right boundary sequences from the *tniB* gene to the IRt using the primer combination TniB-F/IRHP (Table S2). In the case of the Tn*402*-like element found in *P. monteilii* HB157 lacking most of the *tni* module with the exception of *tniC* (see below), the sequence of the right boundary was completed by an inverse PCR procedure (Ochman et al., 1988). In short, 1 μg of genomic DNA from this isolate was digested by *Eco*RI, the resulting fragments were ligated with T4 DNA ligase (Promega), and used as templates in PCR assays performed in 25 μl-reactions containing 0.1 μg of this circularized DNA, 0.5 μM of each VIM-Rf and IRHPr primers (Table S2), 200 μM of each dNTP, 2 mM MgSO4 and 1.0 U Platinum Taq DNA polymerase High Fidelity (Invitrogen, Carlsbad, CA). The amplification bands thus obtained were then ligated to pGEM-T Easy (Promega), and transformed into *E. coli* DH5α cells by electroporation. Plasmids were extracted from different colonies containing inserts and analyzed by restriction mapping and DNA sequencing using the VIM-Rf primer. The right boundary DNA sequence of this Tn*402*-like element was then completed by primer walking with the sequential use of tniC-F and IS6100-F primers (Table S2). The above procedure allowed us to obtain not only the complete sequence of the Tn*402*-like element found in *P. monteilii* HB157 (5239 bp), but also that of a 732 bp fragment located in the immediate vicinity of its insertion site (see below). The combined sequence (5971 bp) was deposited in GenBank under accession number MZ382911.

2.5. Conjugation and transformation assays

Conjugation experiments were performed using the carbapenem-resistant *P. putida* G clinical isolates (Table 1) as donors, and rifampicin-resistant *E. coli* DH5α or rifampicin-resistant *P. aeruginosa* PAO1 cells as recipients (Marchiaro et al., 2010). The transconjugants were selected on LB agar containing 20 μg/ml ampicillin and 150 μg/ml rifampicin in the case of *E. coli* DH5α, or 4 μg/ml ceftazidime and 150 μg/ml rifampicin in the case of *P. aeruginosa* PAO1. The MIC values of these transconjugants towards different antimicrobials were determined as described above. The self-transferability of the plasmids present in the *E. coli* DH5α transconjugants was further tested by agar mating studies (Marchiaro et al., 2010; De Belder et al., 2017) employing as recipient *E. coli* MC4100 harboring the chloramphenicol-resistance plasmid pACYC184 (Marchiaro et al., 2010).

In the cases of *P. putida* G isolates in which no *E. coli* transconjugants could be obtained, plasmid DNA was isolated and used to transform *E. coli* DH5α by chemical ($CaCl_2$) treatment (Sambrok et al., 1989) or *P. aeruginosa* PAO1 by electroporation (Choi et al., 2006), selected on LB agar containing 20 μg/ml ampicillin, or 4 μg/ml ceftazidime, respectively.

The presence of the bla_{VIM-2} gene in the transconjugant or transformant cells obtained as described above was confirmed by PCR and

sequencing analysis (Table S2). Plasmids from *E. coli* DH5α transconjugants were purified (Wizard Plus SV Minipreps DNA Purification System) and furtherly characterized by *Eco*RI digestion/agarose gel electrophoresis. In addition, selected plasmids were subjected to sequencing analysis (see below).

2.6. Plasmid sequencing and comparative sequence analyses

pLA111 and pBA7816 nucleotide sequences were determined on a 454 pyrosequencing platform (Roche Diagnostics Corporation) at the Instituto de Agrobiotecnología Rosario (INDEAR). The obtained contigs were assembled *in silico* using as framework the structure previously determined for pLD209 (Marchiaro et al., 2014). Gaps remaining between contigs were closed by PCR using specifically-designed primer pairs (Table S2), a procedure that was also used to verify the circular structures of the plasmids. In the case of pLA111 we employed the virB10-F/virB8-R primer combination, and for pBA7816, mob-F/mob-R, 7816-F/VIM-R and TniA-F2/REPIR-T3 primer combinations (Table S2).

The DNA sequences of all PCR amplicons and cloned inserts obtained were determined at the University of Maine DNA Sequencing Facility, Orono, USA.

The Rapid Annotation using Subsystem Technology standard operating procedures (RAST, http://rast.nmpdr.org/seedviewer.cgi) (Aziz et al., 2008) and the National Center for Biotechnology Information database (NCBI, U.S. National Library of Medicine, Bethesda MD, USA) were used to annotate the open reading frames (ORFs). Searching for antimicrobial resistance determinants was done using ResFinder 2.1 (https://cge.cbs.dtu.dk/services/ResFinder/; Zankari et al., 2012). The detection of IS was done with ISFinder (Siguier et al., 2006) (https://www-is.biotoul.fr/).

2.7. Target sites of Tn6335 in the chromosome of P. asiatica HP613 and P. putida G/II LA1008

Total genomic DNA from the mentioned isolates (purified using the Wizard Genomic DNA Purification Kit) was digested with EcoRI and ligated to EcoRI-digested pSU18, an *E. coli* cloning vector conferring chloramphenicol resistance. The ligation mixture was transformed into *E. coli* DH5α by electroporation, and transformants carrying inserts containing bla_{VIM-2} were selected on LB agar plates containing ceftazidime (4 μg/ml) and chloramphenicol (25 μg/ml) supplemented with 40 μg/ml X-gal and 54 μg/ml IPTG. Plasmids were extracted from different colonies, and the DNA sequences of the inserts in the vicinity of the EcoRI cloning site of pSU18 were determined employing a primer hybridizing in the multiple cloning site of pSU18 (pSU18-F, Table S2). The sequences of the inserts were then completed by primer walking taking account the sequence information obtained in each case. The EcoRI fragments carrying bla_{VIM-2} cloned by this procedure from *P. asiatica* HP613 and *P. putida* G/II LA1008 were deposited in GenBank under accession numbers MZ382912 and MZ382913, respectively.

3. Results and discussion

3.1. Bacterial isolates

A total of 13 carbapenem-resistant clinical isolates from hospitals of the Buenos Aires City area and Rosario City area of Argentina, identified phenotypically as belonging to the *P. putida* G by the VITEK 2C System, were included in this study (Table 1 and Table S1). All isolates showed clinical resistance to several β-lactams including imipenem and meropenem, and microbiological assays (Marchiaro et al., 2005) confirmed that they possessed MβL activity. Screening for different MβL genes by PCR (bla_{IMP}, bla_{VIM}, bla_{SPM} and bla_{NDM}, Table S2), followed by sequencing analysis of the amplicons found only bla_{VIM-2} in all of the above *P. putida* G isolates.

3.2. Assignment of isolates to the species level

A more precise delimitation of the 13 isolates to the species level among the *P. putida* G was conducted by a MLSA approach employing concatenated partial sequences of 16S rDNA, *gyrB* and *rpoD* genes (Mulet et al., 2010, 2013). Therefore, judging from the percentages of identity of concatenated core gene sequences between the analyzed isolates and assigned representative (type) species of this group, isolates BA7908 and BA9115 were assigned to *P. putida sensu stricto*; isolates LD209, HB313, HP613 and BA7816 to *P. asiatica*; HB157 and BA9713 to *P. monteilii*; and LA111 to *P. juntendi* (Table 1). However, for 4 isolates (HP813, HE1012, BA9605 and LA1008) the observed percentages of identity between core genes concatenates and the closest defined nominated reference species (Table 1) were either lower or very close to the adopted 97% threshold value used to differentiate between species among the *P. putida* G (Mulet et al., 2010, 2013). Moreover, as also seen in Table 1, when judged by the same criterion these isolates were closer to newly proposed *P. putida* G species which have received designations from G/I to G/VI (Mulet et al., 2013). Thus, we decided to adopt the best match for these isolates, and assigned HP813 to *P. putida* G/I; LA1008 and HE1012 to *P. putida* G/II, and BA9605 to *P. putida* G/V (Table 1).

Secondly, a maximum-likelihood (ML) phylogenetic analysis using the corresponding concatenated sequences (Fig. 1) reinforced the above assignation of isolates BA9115 and BA7908 to *P. putida sensu stricto*; HB157 and BA9713 to *P. monteilii*; BA7816, LD209, HP613, and HB313 (the latter three isolates displaying identical concatenate sequences, Table S3) to *P. asiatica*; and LA111 to *P. juntendi*, as judged by the monophyletic groups formed in each case with the corresponding defined species. It is worth noting that strain LD209, previously characterized as a member of the *P. putida* G on the basis of phenotypic procedures (Marchiaro et al., 2014), was now more precisely assigned to *P. asiatica* on the basis of the analysis conducted here.

Similarly, as seen in Fig. 1, HP813 clustered with *P. putida* KT2440 (proposed new species G/I, Mulet et al., 2013); LA1008 and HE1012 with *P. putida* ATCC 23483 (proposed new species G/II, Mulet et al., 2013); and BA9605 with *P. putida* W619 (proposed new species G/V, Mulet et al., 2013). Thus, our local collection of clinical isolates was composed of (at least) seven differentiated species among the *P. putida* group. It is worth noting that in the ML tree (Fig. 1) the RYU5 strain, which was recently proposed as the *P. asiatica* type strain (Tohya et al., 2019a), clustered with the CFBP4966 strain previously assigned to *P. putida* G/IV at the species level (Mulet et al., 2013). Our observations (Fig. 1) suggest that *P. asiatica* and *P. putida* G/IV actually represent the same species within the *P. putida* group.

In summary, we could detect bla_{VIM-2} in seven distinguishable species of the *P. putida* G among the 13 clinical isolates analyzed here, reinforcing the notion of this group acting as reservoir of this carbapenem resistance gene (Marchiaro et al., 2010, 2014). A further and more discriminatory fingerprinting analyses (Limansky and Viale, 2002) showed that the four clinical isolates assigned here to *P. asiatica* (see above) could be additionally subdivided into two separate clonal lineages: one constituted by LD209, HB313, and HP613, and the other by BA7816 (Fig. S1, Table 1). It is worth noting here the persistence of a specific clone of *P. asiatica*, designated Pa_A (Table 1 and Table S1) in our nosocomial environment for an extended period of time. In this context, we observed not only the presence of clonally-related *P. asiatica* isolates such as LD209 and HP613 in the same hospital at different dates, but also an almost simultaneous presence of clonally-related isolates of this species in different hospitals such as HP613 and HB313 (Fig. S1 and Table S1). The two isolates assigned to *P. putida sensu stricto* (BA9115 and BA7908, respectively) could be also separated by this methodology in two separate clonal lineages, and similar situations were found for the two isolates assigned to *P. monteilii* (HB157 and BA9713, respectively) and for the two *P. putida* G/II isolates (LA1008 and HE1012, respectively) (Fig. S1, Table 1). These results indicated the presence of 11 still distinguishable strains among the 13 *P. putida* G isolates included in this

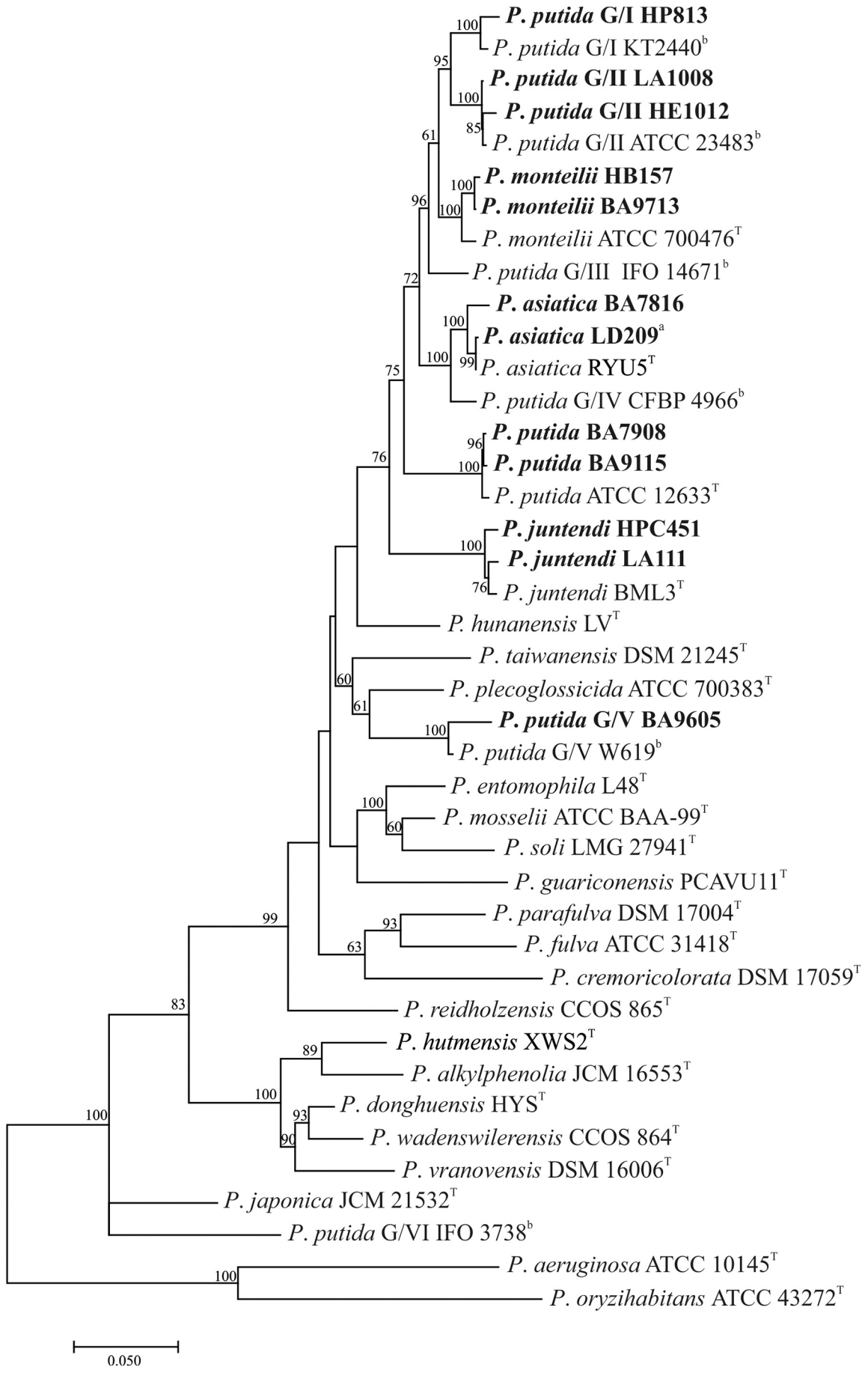

(caption on next page)

Fig. 1. Phylogenetic analysis of the *Pseudomonas putida* G isolates analyzed in this work. A ML phylogenetic tree was constructed from alignments of the concatenated sequences of partial regions of 16S rDNA, and *gyrB* and *rpoD* genes. The *P. putida* G clinical isolates analyzed in this work are in bold. The analysis also incorporates the corresponding concatenated sequences of 21 *P. putida* G type strains which have received species assignation (Mulet et al., 2013; Tohya et al., 2019a, 2019b) as well as from 6 strains representing proposed novel species (*P. putida* G/I to *P. putida* G/VI, indicated by [b] superscripts). The equivalent concatenate sequences of *P. aeruginosa* ATCC 10145^T and *P. orzihabitans* ATCC 43272^T type strains were included as outgroups. Only bootstrap percentages higher than 60% (1000 replicates) are indicated at the nodes. In LD209[a], the superscript indicates the representative isolate of the clonal lineage Pa_A among the *P. asiatica* isolates, which also includes HP613 and HB313 (not shown in the figure) that share with LD209 identical core gene concatenate sequences. In all cases the superscript ^{T} indicate the type strains.

study, and exemplify the difficulties in defining the limits between species in the *P. putida* G (Mulet et al., 2010, 2013; Peix et al., 2018; Tohya et al., 2019a, 2019b). A further characterization of the bla_{VIM-2}-carrying genetic platforms present in these isolates could then shed light on the mechanisms of dissemination of carbapenem-resistance genes among the bacterial population sharing this environment.

3.3. Characterization of genetic structures harboring bla_{VIM-2} genes in the *P. putida* G isolates analyzed

The characterization of the near genomic context of bla_{VIM-2} using PCR primers designed to hybridize in the 5′- and 3′- conserved segments (CS, Int1-F and Int1-R, respectively, Table S2) of "typical" or "*sul1*-type" class 1 In/Tn (Partridge et al., 2018) systematically failed to produce amplification bands when total DNA samples extracted from each the 13 *P. putida* G clinical isolates analyzed here were used as templates. Further sequence analysis (see below) indicated in fact that the In/Tn present in our isolates belong to the "atypical" class lacking the conserved 3'-CS region, thus explaining these amplification failures. Conversely, the use of Int1-F and TniC-R2 primers, which bind to the 5′-CS and the 5′ region of the *tniC* gene located in the *tni* module of Tn*402* transposons, respectively (Table S2) generated amplification bands in all of them. Subsequent sequencing analysis of the amplicons not only confirmed the presence of bla_{VIM-2} gene cassettes and their association to a *tniC* gene in all isolates, but also identified the presence of three different bla_{VIM-2}-containing class 1 integrons among them (Fig. 2).

We have previously reported that the *P. asiatica* LD209 strain carries a conjugative plasmid of 38,403 bp, which was designated pLD209 (Marchiaro et al., 2010, 2014). The detailed analysis of the pLD209 sequence (Marchiaro et al., 2014) indicated that it harbors a Tn*5053*/Tn*402* family transposon of 7633 bp endowed with a complete *tniABQC* module carrying a class 1 integron (In41) possessing bla_{VIM-2} and *aacA4* resistance cassettes (Fig. 2A). This Tn*402* transposon received the designation Tn*6335* by the Tn Number Registry (Tansirichaiya et al., 2019). Sequence characterization of the amplicons obtained from the 13 *P. putida* G isolates described above indicated the presence of the In41 arrangement in 9 isolates of them belonging to 7 different species (Table 1). Further PCR amplification of the immediate genetic context of In41 in these 9 isolates followed by sequencing analysis confirmed the presence of Tn*6335* in all of them.

From the other 4 isolates, only the bla_{VIM-2} gene cassette was found in the variable region of the class 1 integron carried by *P. putida* BA9115 and *P. asiatica* BA7816 (Table 1). This single-cassette integron was previously reported in *Pseudomonas chlororaphis* M11740 (Faccone et al., 2014), and was designated In899 (GenBank accession number KJ668595). The characterization of the genetic context of In899 indicated that it was also embedded in a complete Tn*402* family transposon spanning 6994 bp, which was designated Tn*6336* by the Tn Number Registry (Fig. 2A).

Finally, a similar analysis conducted in *P. monteilii* HB157 (Table 1) indicated the presence of a class 1 integron carrying *dfrB1*, *aacA4* and bla_{VIM-2} gene cassettes, previously designated In528 (Fig. 2B). Further completion of its genetic context by an inverse PCR procedure indicated a Tn*402*-like element spanning 5239 bp (Fig. 2B). This element, designated here as Tn*402*Δ(*tniABQ*), showed a defective *tni* module containing a complete *tniC* gene with an upstream 44 bp remnant of the approximately 60 bp *tniC*/*tniQ* intergenic region. This structure is adjoined (Fig. 2B) by a stretch of 1155 nucleotides encompassing a complete IS*6100* flanked by inversely-oriented 123 bp (IRt) and 152 bp (IRt) segments of the IRt end of Tn*402* transposons (Fig. 2B). A 1003 bp of this fragment that includes the 123-bp IRt′ and adjoining IS*6100* displayed complete identity to an equivalent region of a class 1 In/Tn element designated In4, present in *P. aeruginosa* plasmid R1033 (GenBank accession U12338.3; positions 10,524 to 11,526). In addition, another 1032 bp region encompassing IS*6100* and the adjoining 152 bp IRt-containing fragment showed complete identity to an equivalent region of another class 1 In/Tn element designated In28 present in *P. aeruginosa* plasmid RPL11 (GenBank AF313472.2, positions 8971 to

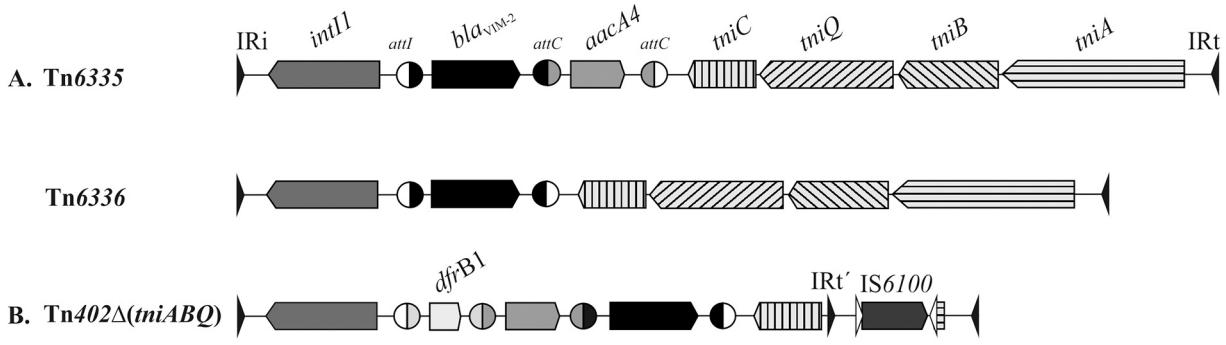

Fig. 2. Genetic organization of bla_{VIM-2}-containing Tn*402*-like class 1 integrons identified in *Pseudomonas putida* G clinical isolates. A. Schematic structure of the class 1 integrons In41 and In899 embedded into complete Tn*402*-like transposons designated Tn*6335* (7633 bp, GenBank accession number KF840720.1) and Tn*6336* (6994 bp, GenBank accession number MN240297.1), respectively. **B**. Same, for the In528 class 1 integron embedded into a Tn*402*-like element lacking most of the *tni* module detected in *Pseudomonas monteilii* HB157 (Tn*402*Δ(*tniABQ*), 5239 bp; GenBank accession number MZ382911). The inverted repeats (IR) associated with the left and right boundaries, respectively, of each transposable element are indicated by oppositely-oriented closed arrows at the corresponding Tn borders. The individual genes are represented by boxed arrows (distinctively labeled in each case) indicating the corresponding directions of transcription. In **B**, a second 25-bp sequence identical to IRt, designated IRt′, was located immediately upstream of the *tniC* gene (black triangle facing IS*6100*). The left inverted repeat (IRl) and right inverted repeat (IRr) of IS*6100* are indicated by the oppositely-oriented open arrows located at the borders of the transposase gene (in dark gray). The figure is not drawn to scale.

10,002). Both In4 and In28 form part of the widely distributed group of In4-like class 1 In/Tn, differing between them in the extent and gene composition of the 3′-CS, the absence of the internal IRt in In28, and the presence of the extra partial copy of IS*6100* in In4 (Partridge et al., 2001). In the case of the Tn*402*Δ(*tniABQ*) element found in *P. monteilii* HB157, the 3′-CS was missing and an IS*6100* (lacking the partial duplication segment found in In4) was found flanked by (internal) IRt′ and (external) IRt inverted repeat sequences (Fig. 2B). Our database searching identified an identical Tn*402*Δ(*tniABQ*) element in the chromosome of *P. putida* PP112420, a clinical strain isolated in China (GenBank accession CP017073.1; nucleotide positions 5,137,406 to 5,142,644). The observation that this Tn*402*Δ(*tniABQ*) element (Fig. 2B) is bounded by IRi and IRt (and immediate associated sequences) characteristic of Tn*5053*/Tn*402* transposons (Kholodii et al., 1995) opens the possibility that it could be mobilized to other genomic locations in cells providing in *trans* the enzymes required for transposition.

3.4. Conjugative transfer of plasmids carrying bla_{VIM-2}-containing Tn402-like class 1 integrons from P. putida G isolates to E. coli and P. aeruginosa laboratory strains

We previously reported that pLD209 harbored by *P. asiatica* LD209 is a conjugative plasmid which could be mobilized from this strain to *E. coli* DH5α or to *P. aeruginosa* PAO1 (Marchiaro et al., 2010). By conducting similar conjugation experiments, we could detect plasmid transfer to these recipients when the donors were *P. asiatica* LD209 (used as control), *P. asiatica* BA7816, *P. asiatica* HB313, *P. putida* G/II HE1012, *P. putida* G/V BA9605, and *P. juntendi* LA111, as judged by the acquisition of imipenem resistance in the corresponding transconjugants and the subsequent detection of acquired MβL activity in all of them (Table S4 and data not shown).

The antimicrobial susceptibility patterns (MIC values) of the corresponding *E. coli* DH5α transconjugants (designated Ect209, Ect7816, Ect313, Ect1012, Ect9605 and Ect111, respectively) are shown in Table S4. As seen in the Table, all of them acquired resistance to imipenem, meropenem, and the other β-lactams tested. Moreover, and with the exception of Ect7816, the MIC values to gentamicin also increased from 4- to 8-fold in these transconjugants (Table S4). These observations are in agreement with the conjugative transfer, from the indicated *P. putida* G isolates, of a plasmid containing Tn*6335* carrying bla_{VIM-2}- and *aacA4*-resistance cassettes in the cases of Ect209, Ect313, Ect1012, Ect9605 and Ect111 transconjugants, and of a plasmid housing Tn*6336* carrying only a bla_{VIM-2} cassette in Ect7816 (Fig. 2A).

To further examine the self-transfer capability of the plasmids selected in each of these Ect transconjugants, agar mating assays were done using each of them as donors, and chloramphenicol-resistant *E. coli* MC4100 cells as recipients following previously described procedures (Marchiaro et al., 2010) (Table 1). The overall results confirmed that the plasmids present in all of the above transconjugants are self-mobilizable, and therefore potentially capable of spreading the bla_{VIM-2} containing-Tn*402*-like element among a wide range of co-existing bacterial species including *P. aeruginosa* and members of the *Enterobacteriaceae*.

The plasmids selected in the above Ect transconjugants were extracted and subjected to restriction mapping with *Eco*RI. With the exception of Ect7816, plasmids derived from Ect1012, Ect9605, Ect313, and Ect111 showed very similar restriction profiles, which were in turn

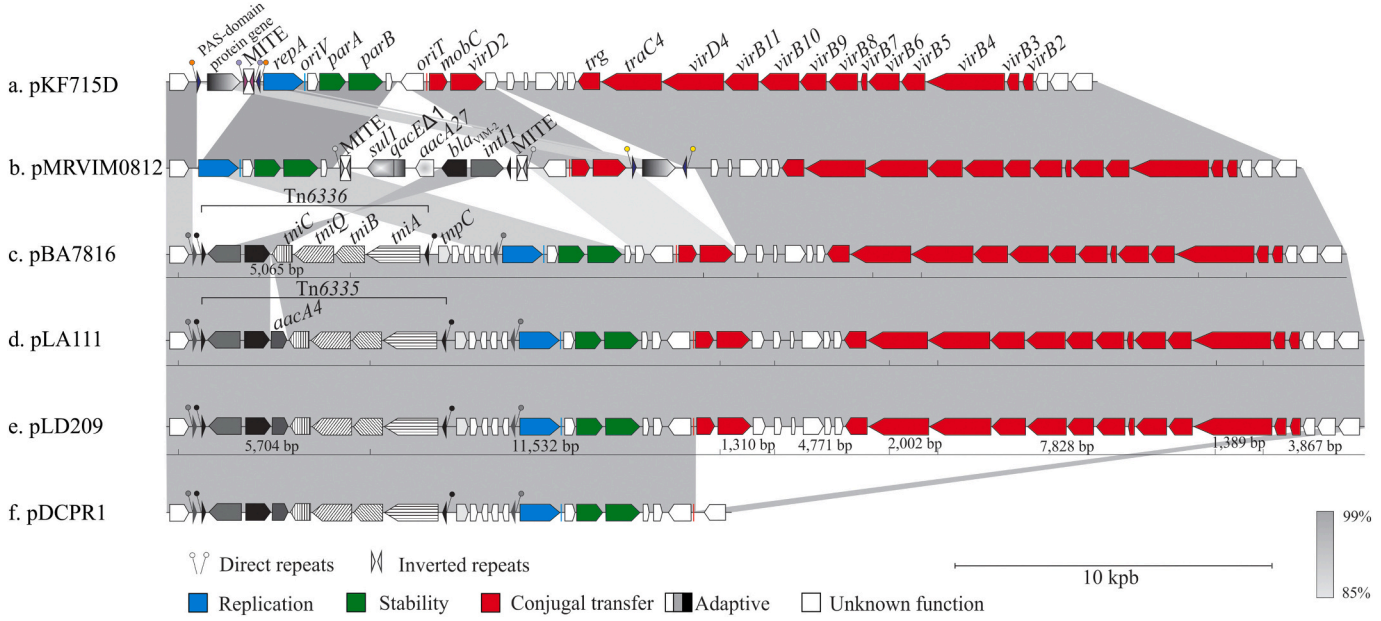

Fig. 3. Comparative analysis of pLD209-type plasmids. Linear representations of the structures of five plasmids detected in databases sharing homology with pLD209 including a) pKF715D (GenBank accession number AP015033.1), b) pMRVIM0812 (CP010893.1), c) pBA7816 (MN240297, this work), d) pLA111 (MT192131, this work), e) pLD209 (KF840720.1), f) pDCPR1 (KJ577613). The regions shaded in gray tones linking the different structures reflect percentages of nucleotide sequence identity ranging from 85% to 99% as detected in a BLASTn search, with the scale depicted at the lower right part of the figure. The positions of *Eco*RI restriction sites inferred from the corresponding DNA sequences are indicated below plasmids pBA7816, pLA111, and pLD209, with the fragment sizes predicted *in silico* shown only for pLD209. A 5-bp 5′-GTTTT-3′ direct duplication (black circles) is present at the immediate outer borders of the 25-bp inverted repeats IRi and IRt (black triangles facing inwards accompanying the black circles) of both Tn*6335* and Tn*6336*. These Tn*402*-like elements are flanked by an external 34-bp inverted repeat (5′-GGGGGTGTAAGCCGGAACCCCAGAAAATTCCGTC-3′, gray triangles facing inwards), with one extreme (IRl) located immediately upstream of IRi and its complementary (IRr) located immediately upstream of the *repA* gene. These external IR sequences are bordered by a 5′-TATTC-3′ direct repeat (gray circles accompanying the gray triangles). The single MITE element in pKF715D is located between nucleotide positions 20,221 to 20,482, and is flanked by a 5-bp direct repeat, 5′-AACTT-3′ (violet circles). The two MITE elements in pMRVIM0812 are located between positions 27,596–27,858 and 32,920-33,182, respectively, and the resulting composite transposon-like structure is flanked by the 5-bp direct repeat 5′-GATGA-3′ (light gray circles). The PAS-domain protein coding gene and adjacent MITE element in pKF715D are limited by a 50-bp inverted repeat, and flanked in turn by a 5-bp direct repeat, 5′-AGGAA-3′ (orange circles). In pMRVIM0812, the PAS-domain protein gene is also limited by a 50-bp inverted repeat flanked in turn by a 5-bp direct repeat, 5′-TGGAT-3′ (yellow circles). (For interpretation of the references to colour in this figure legend, the reader is referred to the web version of this article.)

very similar to those of Ect209 (data not shown, see also below). Moreover, the obtained sizes corresponded closely to the EcoRI fragment sizes predicted *in silico* from the pLD209 complete DNA sequence (Fig. 3e; Marchiaro et al., 2014). The plasmids purified from Ect7816 (henceforth, pBA7816) and Ect111 (henceforth, pLA111) were subjected to further sequencing for comparative structural analysis. pLA111 (GenBank accession number MT192131) was 99.9% identical to pLD209 (Fig. 3d and e, respectively), in agreement with the restriction analysis mentioned above. In turn, pBA7816 (Fig. 3c, GenBank accession number MN240297) was almost identical (99%) to pLD209, their only main difference residing between the corresponding adaptive modules and consisting in the absence of the *aacA4* aminoglycoside resistance cassette (Fig. 2A and Fig. 3). It is worth noting that Tn*6336* and Tn*6335* are positioned in equivalent positions in these plasmids, that they are bordered by the same 5-bp DR (5′-GTTTT-3′), and that they are inserted within another potential mobile element as judged by the external 34-bp inverted repeats (5'-GGGGGTGTAAGCCGGAACCCCAGAAAATTCC GTC-3′, gray triangles facing inwards) and accompanying direct repeats located upstream of the IRi and downstream of the IRt (Fig. 3). Our BLASTn search of the NCBI bacterial DNA database (as for October 9, 2020) using as query the pLD209 sequence (KF840720.1) found 99% nucleotide identity between a fragment of 1861 bp from this plasmid with a fragment extending 1802 bp present in plasmid p3 of an environmental *Pseudomonas koreensis* strain, P19E3 (GenBank accession CP027480.1, positions 265,881 to 264,070). This region in *P. koreensis* p3 covered exactly an element bordered by identical 34-bp inverted repeats, and also similar hypothetical protein coding sequences than those found in pLD209 after removing *in silico* the Tn*6335* insertion at the 5′-GTTTT-3′ direct repeat (122 bp from the IRi, from positions 891 to 1012, and 1739 bp from the IRt, from positions 8651 to 10,389 in KF840720.1; see also Marchiaro et al., 2014). These observations strongly suggest that a similar mobile external element was collected by a pLD209 ancestor, probably as the result of a *trans*-mediated transposition event, and subsequently targeted by a Tn*402*-like transposon thus generating the backbone of the adaptive module now observed in pLD209 and related plasmids (Fig. 3).

Concerning the other seven *P. putida* G isolates analyzed, *i.e.*, *P. asiatica* HP613, *P. putida* BA9115, *P. putida* BA7908, *P. monteilii* BA9713, *P. monteilii* HB157, *P. putida* G/I HP813, and *P. putida* G/II LA1008, repeated attempts to detect plasmids by either conjugation or transformation were unsuccessful. This indicated that the Tn*402*-like elements harboring bla_{VIM-2} in these *P. putida* G isolates (Fig. 2) are located in genome regions other than pLD209-related plasmids, suggesting in turn that they had transposed to these locations after these plasmids accessed their novel hosts (see also below).

3.5. Identification in bacterial database sequences of plasmids structurally related to pLD209

Our BLASTn search using the pLD209 sequence as a query (see above) detected two plasmids, pKF715D and pMRVIM0812, showing high levels of nucleotide identity and structural organization with pLD209, including the replication, stability, and transfer modules (Fig. 3). pKF715D (Fig. 3a) was found in an environmental *P. putida* strain, KF715 (Suenaga et al., 2017), and differs from the other plasmids in that it lacks antimicrobial resistance genes. pMRVIM0812 (Fig. 3b), which was found in a clinical *Pseudomonas* isolate, also contains an adaptive module carrying bla_{VIM-2}. However, and contrasting pLD209, the carbapenemase gene is embedded in a typical class 1 integron also encompassing an aminoglycoside 6′-acetyltransferase *aacA27* gene cassette accompanied by a 3'-CS that includes *qacEΔ1-sul1* genes. A similar class 1 integron, designated In984, was previously described in a clinical *Pseudomonas oleovorans* isolate, M13320 (Faccone et al., 2014, GenBank accession number KJ668596). In pMRVIM0812, In984 is flanked by two copies of miniature inverted-repeat transposable elements (MITEs), the whole structure bordered in turn by a 5-bp (5′-GATGA-3′) direct repeat (Fig. 3b). MITEs are non-autonomous mobile elements bounded by inverted repeats, and their mobilization is promoted by transposases encoded either by adjacent transposons or ISs displaying similar repeats (Bardaji et al., 2011; Delihas, 2011). The whole assembly suggests that these MITE elements captured the integron in a composite transposon-like structure, which was subsequently mobilized to its present location in a pMRVIM0812 predecessor by transposases provided in *trans*. Similar capturing and transposing events of other class 1 integrons by flanking MITE elements have been recognized as a mechanism for mobilizing antimicrobial resistance determinants (Gillings et al., 2009).

Both pMRVIM0812 and pKF715D also carry each a PAS-domain protein coding sequence (Fig. 3, a and b), which are important signaling sensors that monitor changes in light, redox potential, oxygen, and overall energy level of a cell (Taylor and Zhulin, 1999). In the former is bordered by a 50-bp inverted repeat while in the latter is adjacent to a MITE element with the whole arrangement flanked in turn by a 50-bp inverted repeat. In both cases the inverted repeats are flanked in turn by 5-bp direct repeats (Fig. 3, a and b), reinforcing the notion that these PAS-domain sequences and associated elements most probably reached their present locations in the plasmids following also the assistance of *trans* factors provided during transit through different bacterial hosts.

Finally, evidence exists that the above structurally related plasmids can evolve not only by gaining different genetic elements but also by losing significant parts of their backbones, a situation exemplified by pDCPR1 (Fig. 3f) isolated from clinical strains of both *P. aeruginosa* and *Serratia marcescens* in Argentina (Vilacoba et al., 2014). pDCPR1 shares high structural and nucleotide similarity to pLD209 at the adaptive, replication, and stability modules, but lacks most genes involved in conjugal transfer (Fig. 3). Still, the retention of *oriT* sequences suggests that it could still be mobilized when co-existing with a conjugative plasmid providing the appropriate missing functions in *trans*. The structural rearrangements found in pDCPR1 are most likely adaptive consequences associated with lateral transfer, and reinforce the role of pLD209-related plasmids as efficient and plastic genetic platforms for the spreading of carbapenem (and other antimicrobial resistance genes) among different nosocomial pathogens (Marchiaro et al., 2014; Vilacoba et al., 2014).

3.6. Transposition of bla_{VIM-2}-containing Tn*402*-like transposons to selected targets in different *P. putida* G species

We described above that Tn*6335* and Tn*6336* were carried by pLD209-type conjugative plasmids in six of the 13 *P. putida* G isolates characterized here, but resided in a different genome location in the other seven isolates (Table 1). Remarkably, this situation applied for isolates belonging to a same species such as *P. putida* G/II HE1012 and LA1008, and even to a same clonal lineage within a given species such as *P. asiatica* LD209 and HP613 (Table 1). This suggested that the bla_{VIM-2}-containing Tn*402*-like elements characterized here were capable to transpose intracellularly from their original location to other sites of the genome. This represents a most worrying scenario, since it allows in principle the preservation of the bla_{VIM-2} gene even in conditions in which the incoming plasmid fails to replicate in a novel host.

Database searching analysis and experimental evidence with plasmid model systems have identified a high selectivity of Tn*5053*/Tn*402* family members for targets clustered in, or close to, the *res* regions located upstream of a *tnpR* resolvase gene of Tn*21* subgroup members of the Tn*3* family, or the equivalent *par* regions associated with segregational mechanisms of particular plasmids (Betteridge et al., 2011; Gillings, 2014; Kamali-Moghaddam and Sundström, 2000; Minakhina et al., 1999; Nicolas et al., 2015; Papagiannitsis et al., 2017, 2020; Partridge et al., 2018; Petrovski and Stanisich, 2010). While Tn*5053*/Tn*402* transpositions independent of the presence of a *res* or a *par* locus have also been found, the frequencies are very low and involve random

target selection (Petrovski and Stanisich, 2010; Shapiro and Sporn, 1977). It is worth noting in the last context that Tn*6335* was found in pLD209 with the 5-bp DR at its border characteristic of a transposition event, and that insertion occurred in a defective element that was in turn bordered by 34-bp inverted repeats (Marchiaro et al., 2014). However, no sequences resembling *res* or *par* target sites could be identified in the vicinity of the insertion site (Fig. 3). This suggests that, either the acquisition of this transposon by pLD209 resulted from an unusual transposition event, or that substantial sequence rearrangements occurred after transposition near the insertion site, a situation reported in other cases (Kamali-Moghaddam and Sundström, 2000; Partridge et al., 2018; Rådström et al., 1994).

To identify targets of bla_{VIM-2}-containing Tn*402*-like transposons in the genomes of the *P. putida* G species described here, we characterized first the genomic context of Tn*6335* in *P. asiatica* HP613 and in *P. putida* G/II LA1008 (Table 1). The cloning of the insertion region next to the IRi boundary of Tn*6335* on the genome of these isolates was therefore attempted, taking advantage of the nearby bla_{VIM-2} gene and the single *Eco*RI site within its *tniB* gene (Fig. 3). In short, we digested total genomic DNA from each of these isolates with EcoRI, ligated the digested products into EcoRI-digested pSU18, transformed *E. coli* DH5α cells, and selected for colonies containing inserts that, besides the chloramphenicol resistance provided by pSU18, conferred ceftazidime resistance provided by the bla_{VIM-2} gene. Different clones were then subjected to plasmid purification and sequencing analysis of the inserts.

In the case of *P. asiatica* HP613, this procedure consistently recovered a 9031-bp EcoRI insert cloned into pSU18 (GenBank accession number: MZ382912; pSU18-HP613; Fig. S2A). This fragment encompassed the expected 5307 bp region of Tn*6335* containing the bla_{VIM-2} gene that extended from the IRi to the EcoRI site located 406-bp of the 3′end of *tniB*, plus a 3725 bp of the HP613 genome spanning from the IRi boundary of the transposon to a nearby EcoRI site. A BLASTn search using the latter HP613 genome fragment as a query indicated 97.8% nucleotide identity with a *tnpRA* region encoding the serine recombinase (resolvase, *tnpR*) and transposase (*tnpA*) genes of a Tn*501* transposon previously described in plasmid pVS1 from a *P. aeruginosa* isolate (GenBank accession number Z00027.1, nucleotide positions 4620 to 8343; Fig. S2A). Tn*501* forms part of the Tn*21* subgroup of the Tn*3* transposon family (Nicolas et al., 2015; Partridge et al., 2018), in which the *tnpRA* genes are transcribed in the same direction and are preceded by a *res* region composed of *resI*, *resII* and *resIII* subsites (Nicolas et al., 2015; Partridge et al., 2018; Rogowsky et al., 1985; Stokes et al., 2007). Our comparative sequence analysis indicated that the *resI* subsite of the Tn*501*-like element located in the *P. asiatica* HP613 genome had in fact been interrupted by Tn*6335*, with the IRi of the transposon facing the *tnpR* gene (Fig. S2B).

In the case of *P. putida* G/II LA1008, a similar cloning procedure resulted in the recovery of a 9749-bp EcoRI fragment cloned into pSU18 (GenBank accession number: MZ382913; pSU18-LA1008, Fig. S2C). Subsequent sequence analysis indicated the expected 5307-bp internal fragment of Tn*6335* carrying bla_{VIM-2}, accompanied in this case by a 4442 bp fragment of the LA1008 genome spanning from the IRi boundary of the transposon to a nearby EcoRI site (Fig. S2C). A BLASTn search using this LA1008 genome fragment as a query found 99% nucleotide identity with a similar region in the chromosome of *P. putida* H8234 (GenBank accession CP005976.1; positions 3,173,668 to 3,178,100; Molina et al., 2013), and also with a stretch of around 3790 bp in plasmid RPL11 of a *P. aeruginosa* isolate (GenBank accession AF313472). This common 3790 bp fragment, located near the Tn*6335* insertion in LA1008, includes a complete *tnpRA* module (Fig. S2C) and downstream IRr boundary corresponding to a Tn*1403* transposon (Stokes et al., 2007), which belongs also to the Tn*21* subgroup of the Tn*3* family (Nicolas et al., 2015). The remaining fragment of around 650 bp towards the EcoRI site in the LA1008 genome, which shows almost complete nucleotide identity to the equivalent region in the *P. putida* H8234 chromosome, includes 124 bp of the 3′ coding region of a *sdhC* gene (375 bp in length, GenBank accession AGN79094.1) encoding the cytochrome *b*556 subunit of the succinate dehydrogenase (Fig. S2C). Concerning the target region interrupted by Tn*6335* in LA1008, our comparative sequence analysis (Fig. S2D) indicated that the insertion occurred between the *resI* and *resII* subsites located immediately upstream of the *tnpR* gene of the Tn*1403*-like element, with the IRi boundary of Tn*6335* facing the recombinase gene. It is worth noting that the *tnpRA* transposition modules of the Tn*501*-like and Tn*1403*-like elements showed 86% nucleotide identity between them, and differed in the length of the corresponding *tnpR* genes which were 561- and 618-bp, respectively (MZ382912, MZ382913). This situation has been described previously for Tn*21* subgroup members of the Tn*3* family (Nicolas et al., 2015; Rogowsky et al., 1985).

We also found of interest to characterize the insertion site of the bla_{VIM-2}-containing Tn*402*Δ(*tniABQ*) element identified in *P. monteilii* HB157 (MZ382911; Table 1 and Fig. 2B). Using an inverse PCR approach, we could identify in this case a 732 bp fragment corresponding to the immediate vicinity of the IRt border of Tn*402*Δ(*tniABQ*) in its insertion site in the HB157 genome (Fig. S2E). A BLASTn search and comparative sequence analysis (Fig. S2E) indicated that this fragment encompassed a complete *tnpR* resolvase gene of 615 bp followed by the 5′ region of an aminoglycoside O-phosphotransferase gene (*aph*(*3″*)-Ib or *strA*). This 615 bp fragment showed a high percentage of identity with equivalent segments found in the genomes of different *Pseudomonas* species including the chromosome of *P. aeruginosa* FDAARGOS_570 (GenBank CP033835.1, positions 3,824,646 to 3,825,377), in a plasmid carried by the same strain (CP033834.1, positions 25,649 to 26,380), in plasmid p420352-strA of *P. putida* 15,420,352 (MT074087.1, positions 126,666 to 131,160), and in plasmid pPMK1-C of *Klebsiella pneumoniae*, plasmid pRHBSTW-00444_2 of *Citrobacter freundii* RHBSTW-00444, and in the chromosome of *Stenotrophomonas maltophilia* SM 866. In all of the above genomes the identified fragments form part of a transposon designated Tn*5393*c, fully characterized in *Aeromonas salmonicida* (L'Abée-Lund and Sørum, 2000) and originally described in *Erwinia amylovora* (Chiou and Jones, 1993). Tn*5393*-like transposons are ubiquitous members of the Tn*3* family generally carrying streptomycin resistance genes, differing from Tn*21* members in that the *tnpR* gene is separated from an oppositely-oriented *tnpA* gene by a short intergenic region of around 100 bp containing the *res* subsites (Blake et al., 1995; Chiou and Jones, 1993; L'Abée-Lund and Sørum, 2000; Nicolas et al., 2015). Our analysis indicated that Tn*402*Δ(*tniABQ*) was located between the *resII* and *resIII* subsites of the Tn*5393*c-like element present in the *P. monteilii* HB157 genome, with the IRt boundary facing the *tnpR* resolvase gene (Figs. S2E, 2F).

The results presented here indicated that the *res* regions of Tn*3* family transposons present in the genomes of different *P. putida* G species have been preferential targets of Tn*402*-like elements carrying bla_{VIM-2}, which may have been originally acquired by these cells as passengers of pLD209-type conjugative plasmids. This resembles the cases of high-risk MDR clones of *P. aeruginosa*, in which not only bla_{VIM-2} genes but also other carbapenemase genes such as bla_{IMP} and bla_{GES} have been found in association with Tn*3* family elements integrated in the corresponding chromosomes (Botelho et al., 2018a, 2018b; Gillings, 2014; Jeong et al., 2009; Lee et al., 2002; Molina-Mora et al., 2021; Minakhina et al., 1999; Nicolas et al., 2015; Papagiannitsis et al., 2017, 2020; Partridge et al., 2001, 2018; Perez et al., 2014; Van der Zee et al., 2018; Yoon and Jeong, 2021). Carbapenem therapy was probably the main force behind the selection of *P. putida* G clonal lineages in which transposition events relocated the incoming bla_{VIM-2}-containing Tn*402*-like elements, and further rearrangements may have help stabilizing these hybrid structures in the genomes of the new hosts. This predisposition of Tn*5053/402* family members for the *res* regions located on some Tn*3* family members can certainly provide access to alternative and more efficient vehicles of dissemination in bacterial populations sharing similar environmental niches, including the human microbiota (Gillings et al., 2015; Nicolas et al., 2015; Papagiannitsis et al., 2017,

2020; Partridge et al., 2018; Tato et al., 2010). These chimeras could then have played important roles in the further dissemination of *bla*$_{VIM-2}$ genes to pathogenic species causing infections in the clinical setting including *P. aeruginosa* and members of the *Enterobacteriaceae* family such as *S. marcescens* and *Enterobacter* sp. (Vilacoba et al., 2014; De Belder et al., 2017; Izdebski et al., 2018). In this context, we recently isolated from a local hospital a *P. aeruginosa* clinical strain, PAE868 (Table S1), harboring a conjugative plasmid designated pPAE868 (Table S4) different from pLD209 (data not shown), but still carrying the Tn*6335* transposon characterized above.

4. Conclusions

The results of this work emphasize the ability of *P. putida* G members to adapt and survive in the nosocomial setting. The searching of genetic elements containing *bla*$_{VIM-2}$ among different carbapenem-resistant members of the *P. putida* G isolated from hospitals in two cities of Argentina revealed the presence of three Tn*402*-like class 1 integrons (Fig. 2) carrying this resistance gene. These *bla*$_{VIM-2}$-containing Tn*402*-like elements were carried by pLD209-related plasmids in some isolates (Table 1), and are thus capable of inter-cellular mobilization as passengers of these conjugative plasmids (Fig. 4). Besides this mechanism of acquisition in association to conjugative plasmids, we also provide in this work evidences that these Tn*402*-like elements are capable to transpose to *res* target regions of particular Tn*3* family members pre-existing in the genomes of these strains (Fig. 4; a, c and d). The resulting chimeras certainly represent another powerful mechanism of *bla*$_{VIM-2}$- dissemination, not only among *P. putida* G members but also among other bacterial populations sharing the same niches including the clinical setting (Fig. 4e).

The plasticity inherent to the integron carried by the Tn*402* element can also explain the generation of Tn*6336* from Tn*6335* (or *vice-versa*), which only differ in a *aacA4* resistance cassette (Fig. 2). This genetic event may have been selected in a *P. putida* G member (Fig. 4b), possibly in different opportunities, as suggested by the presence of these closely related transposons in different species of the group (Table 1). Also, plasmids such as pPAE868 carrying Tn*6335* could have been generated during the co-existence of a plasmid and the transposon in different locations of a same cell (Fig. 4d), prior to the horizontal transfer of the modified plasmid to *P. aeruginosa* (Fig. 4e). Finally, another possibility of dissemination of the *bla*$_{VIM-2}$-containing Tn*402*-like transposons is provided by plasmids that, with the exception of the replication and adaptive modules, have lost most other parts of their original structures (Fig. 4f). Examples are provided by pLD209-derived plasmids recovered from clinical strains of *S. marcescens* and *P. aeruginosa* (Fig. 3f), which have lost the conjugation module components with the exception of the *oriT* (Vilacoba et al., 2014), and could therefore be mobilized from a *P. putida* G reservoir providing that the missing transfer functions are provided in *trans* (Fig. 4g).

In summary, the observations of this work reinforce our previous proposals that *P. putida* G members are in fact reservoirs of *bla*$_{VIM-2}$-containing Tn*402*-like class 1 In/Tn, which are mobilized intercellularly with the assistance of pLD209-type plasmids (Marchiaro et al., 2010, 2014). This, in addition to their ability to transpose to selected targets on the genomes of their new hosts may help explaining the vast dissemination of *bla*$_{VIM-2}$ carbapenem resistance genes not only among *P. putida* G members, but also among pathogens including *P. aeruginosa* and members of the *Enterobacteriaceae* sharing the clinical niche.

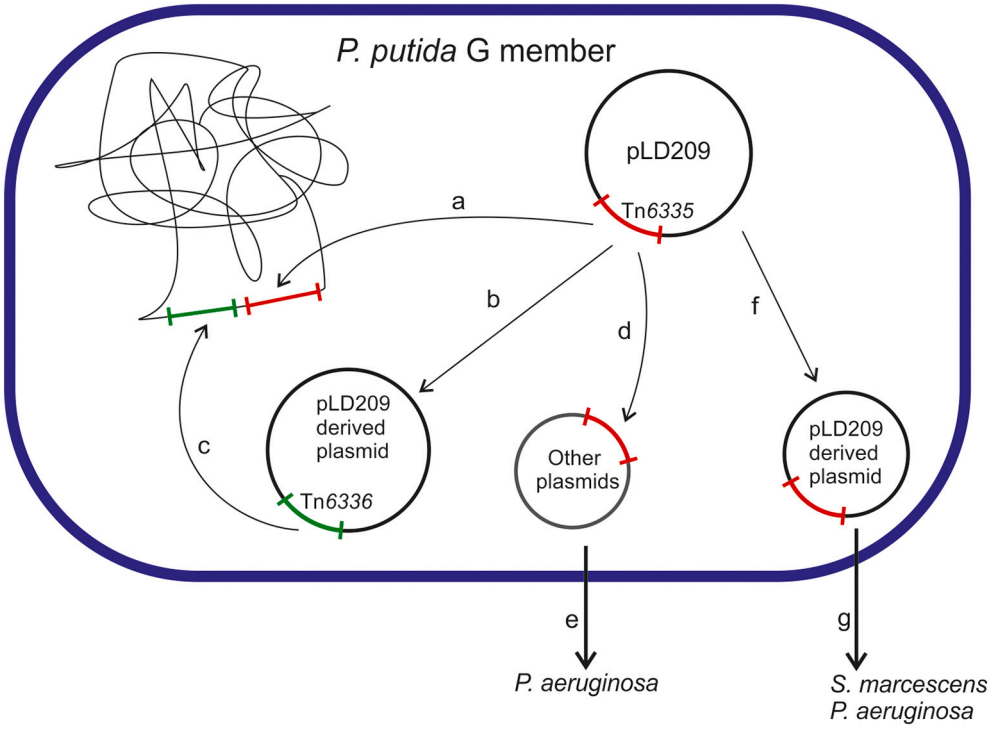

Fig. 4. Proposed routes of intra- and inter-genomic dissemination of *bla*$_{VIM-2}$-containing Tn*402*-like transposons in members of the *Pseudomonas putida* G and other groups of clinical bacteria. Tn*6335* was probably acquired by *P. putida* G members as a passenger of conjugative, pLD209-related plasmids. The incoming plasmid could have persisted in the new host, or could have failed to accompany its replication rate and consequently lost. In the latter case, however, carbapenem pressure could have selected bacterial clones in which the *bla*$_{VIM-2}$-containing Tn*402*-like element had transposed from the incoming plasmid to pre-existing preferred locations located either in the chromosome (pathway a) or in other plasmids (pathway d) such as the *res* sites of Tn*21* subgroup transposons (exemplified in this work by the cases of *P. asiatica* HP613 or *P. putida* G/II LA1008). In turn, the lack of aminoglycoside pressure could have selected clones in which the *aacA4* gene cassette was lost from Tn*6335*, resulting in a pLD209-related plasmid now harboring a Tn*6336* element (b) exemplified here in the case of *P. asiatica* BA7816, and the possibility of this Tn to be located in another region of the genome (c) (*e.g.* BA9115). Transposition of *bla*$_{VIM-2}$-containing Tn*402*-like transposons to a co-habitant conjugative plasmid other than pLD209 (d) could also allow dissemination of *bla*$_{VIM-2}$ by horizontal transfer to other bacterial species, exemplified here by the finding of such a plasmid in a local *P. aeruginosa* clinical isolate, PAE868 (e). Finally, substantial deletions on pLD209 structure may have resulted in the selection of plasmids lacking self-transferability, exemplified by pDCPR1 (f). Since pDCPR1 still preserved the *oriT* region (Fig. 3), its passenger Tn*402*-like element could still be transferred if appropriate conjugation functions are provided in *trans* (g), exemplified by the isolation of this plasmid from *P. aeruginosa* and *Serratia marcescens* clinical strains (Vilacoba et al., 2014).

4.1. Nucleotide sequence accession numbers in GenBank

The nucleotide sequence accession numbers of 16S rDNA, *gyrB* and *rpoD* partial genes from *P. putida* G strains of this study deposited in GenBank are indicated in Table S3. The sequence of the Tn*402*Δ(*tniABQ*) element found in *P. monteilii* HB157 was deposited under accession number MZ382911. The complete nucleotide sequences of plasmids pLA111 and pBA7816 have been deposited under accession numbers MN240297 and MT192131, respectively.

The nucleotide sequences of the fragments cloned into pSU18 carrying the bla_{VIM-2} gene derived from the HP613 and LA1008 genomes have been deposited under accession numbers MZ382912 and MZ382913, respectively.

Supplementary data to this article can be found online at https://doi.org/10.1016/j.meegid.2021.105131.

Author contributions

P.M.M, A.S.L and A.M.V. conceived and designed the work. M.A.B., M.S.·D, and D·F conducted the experimental work. M.A.B. and A.M.V. conducted the bioinformatic analyses. All authors analyzed the data and contributed to the redaction of the manuscript. All authors read and approved the final version of the manuscript.

Credit author statement

Patricia M. Marchiaro, Adriana S. Limansky and Alejandro M. Viale conceived and designed the work. Marco A. Brovedan, María S. Díaz and Diego Faccone conducted the experimental work. Marco A. Brovedan and Alejandro M. Viale conducted the bioinformatic analyses. All authors analyzed the data and contributed to the redaction of the manuscript. All authors read and approved the final version of the manuscript.

Declaration of Competing Interest

None.

Acknowledgments

We are grateful to the personnel of the Bacteriology Service from Hospital Provincial, Hospital Español, and Sanatorio Los Arroyos, Rosario; and Hospital Escuela Eva Perón, Granadero Baigorria, Argentina for kindly providing *P. putida* G clinical isolates. P.M.M. and A.S.L. are Researchers of the National University of Rosario. A.M.V. and D.F. are Careers Researchers of CONICET. M.A.B. is Fellow of CONICET. F.P. and A.C. are Researchers of the Malbrán Institute, Buenos Aires.

This work was supported by grants from the Agencia Nacional de Promoción Científica y Tecnológica (ANPCyT; PICT 2019-00074 to A.S.L., and PICT 2015-1072 to A.M.V.); Consejo Nacional de Investigaciones Científicas y Técnicas (CONICET); Secretaría de Ciencia, Tecnología e Innovación, Provincia de Santa Fe; and Secretaría de Salud Pública, Municipalidad de Rosario.

References

Almuzara, M., Radice, M., Gárate, N., Kossman, A., Cuirolo, A., Santella, G., Famiglietti, A., Gutkind, G., Vay, V., 2007. VIM-2-producing *Pseudomonas putida*, Buenos Aires. Emerg. Infect. Dis. 13, 668–669. https://doi.org/10.3201/eid1304.061083.

Aziz, R.K., Bartels, D., Best, A.A., DeJongh, M., Disz, T., Edwards, R.A., et al., 2008. The RAST server: rapid annotations using subsystems technology. BMC Genomics 9, 75. https://doi.org/10.1186/1471-2164-9-75.

Bardaji, L., Pérez-Martínez, I., Rodríguez-Moreno, L., Rodríguez-Palenzuela, P., Sundin, G.W., Ramos, C., et al., 2011. Sequence and role in virulence of the three plasmid complement of the model tumor-inducing bacterium *Pseudomonas savastanoi* pv. *savastanoi* NCPPB 3335. PLoS One 6 (10), e25705. https://doi.org/10.1371/journal.pone.0025705.

Betteridge, T., Partridge, S.R., Iredell, J.R., Stokes, H.W., 2011. Genetic context and structural diversity of class 1 integrons from human commensal bacteria in a hospital intensive care unit. Antimicrob. Agents Chemother. 55 (8), 3939–3943. https://doi.org/10.1128/aac.01831-10.

Blake, D.G., Boocock, M.R., Sherratt, D.J., Stark, W.M., 1995. Cooperative binding of Tn*3* resolvase monomers to a functionally asymmetric binding site. Curr. Biol. 5 (9), 1036–1046. https://doi.org/10.1016/s0960-9822(95)00208-9.

Bogaerts, P., Bouchahrouf, W., Lissoir, B., Denis, O., Glupczynski, Y., 2011. IMP-13-producing *Pseudomonas monteilii* recovered in a hospital environment. J. Antimicrob. Chemother. 66, 2434–2440. https://doi.org/10.1093/jac/dkr294.

Botelho, J., Grosso, F., Quinteira, S., Brilhante, M., Ramos, H., Peixe, L., 2018a. Two decades of bla_{VIM-2}-producing *Pseudomonas aeruginosa* dissemination: an interplay between mobile genetic elements and successful clones. J. Antimicrob. Chemother. 73 (4), 873–882. https://doi.org/10.1093/jac/dkx517.

Botelho, J., Roberts, A.P., León-Sampedro, R., Grosso, F., Peixe, L., 2018b. Carbapenemases on the move: it's good to be on ICEs. Mob. DNA 9 (37). https://doi.org/10.1186/s13100-018-0141-4.

Chiou, C.S., Jones, A.L., 1993. Nucleotide sequence analysis of a transposon (Tn*5393*) carrying streptomycin resistance genes in *Erwinia amylovora* and other gram-negative bacteria. J. Bacteriol. 175 (3), 732–740. https://doi.org/10.1128/jb.175.3.732-740.1993.

Choi, K.H., Kumar, A., Schweizer, H.P., 2006. A 10-min method for preparation of highly electrocompetent *Pseudomonas aeruginosa* cells: application for DNA fragment transfer between chromosomes and plasmid transformation. J. Microbiol. Methods 64, 391–397. https://doi.org/10.1016/j.mimet.2005.06.001.

Clinical and Laboratory Standards Institute (CLSI), 2019. Performance Standards for antimicrobial susceptibility testing. Twenty-nine informational supplement. Document M100-S24. CLSI, Wayne, PA.

De Belder, D., Faccone, D., Tijet, N., Melano, R.G., Rapoport, M., Petroni, A., Lucero, C., Pasteran, F., Corso, A., Gomez, S.A., 2017. Novel class 1 Integrons and sequence types in VIM-2 and VIM-11-producing clinical strains of *Enterobacter cloacae*. Infect. Genet. Evol. 54, 374–378. https://doi.org/10.1016/j.meegid.2017.07.019.

Delihas, N., 2011. Impact of small repeat sequences on bacterial genome evolution. Genome Biol Evol 3, 959–973. https://doi.org/10.1093/gbe/evr077.

Faccone, D., Pasteran, F., Albornoz, E., Gonzalez, L., Veliz, O., Prieto, M., Bucciarelli, R., Callejo, R., Corso, A., 2014. Human infections due to *Pseudomonas chlororaphis* and *Pseudomonas oleovorans* harboring new bla_{VIM-2}-borne integrons. Infect. Genet. Evol. 28, 276–277. https://doi.org/10.1016/j.meegid.2014.10.012.

Gillings, M.R., 2014. Integrons: past, present, and future. Microbiol. Mol. Biol. Rev. 78, 257–277. https://doi.org/10.1128/MMBR.00056-13.

Gillings, M.R., Labbate, M., Sajjad, A., Giguère, N.J., Holley, M.P., Stokes, H.W., 2009. Mobilization of a Tn*402*-like class 1 integron with a novel cassette array via flanking miniature inverted-repeat transposable element-like structures. Appl. Environ. Microbiol. 75 (18), 6002–6004. https://doi.org/10.1128/AEM.01033-09.

Gillings, M.R., Paulsen, I.T., Tetu, S.G., 2015. Ecology and evolution of the human microbiota: fire, farming and antibiotics. Genes (Basel) 6, 841–857. https://doi.org/10.3390/genes6030841.

Izdebski, R., Baraniak, A., Zabicka, D., Sekowska, A., Gospodarek-Komkowska, E., Hryniewicz, W., Gniadkowski, M., 2018. VIM/IMP carbapenemase-producing *Enterobacteriaceae* in Poland: epidemic *Enterobacter hormaechei* and *Klebsiella oxytoca* lineages. J. Antimicrob. Chemother. 73 (10), 2675–2681. https://doi.org/10.1093/jac/dky257.

Jeong, J.H., Shin, K.S., Lee, J.W., Park, E.J., Son, S.Y., 2009. Analysis of a novel class 1 integron containing metallo-beta-lactamase gene VIM-2 in Pseudomonas aeruginosa. J. Microbiol. 47 (6), 753–759. https://doi.org/10.1007/s12275-008-0272-2.

Juan, C., Zamorano, L., Mena, A., Albertí, S., Pérez, J.L., Oliver, A., 2010. Metallo-β-lactamase-producing *Pseudomonas putida* as a reservoir of multidrug resistance elements that can be transferred to successful *Pseudomonas aeruginosa* clones. J. Antimicrob. Chemother. 65, 474–478. https://doi.org/10.1093/jac/dkp491.

Kamali-Moghaddam, M., Sundström, L., 2000. Transposon targeting determined by resolvase. FEMS Microbiol. Lett. 186, 55–59. https://doi.org/10.1111/j.1574-6968.2000.tb09081.x.

Kholodii, G.Y., Mindlin, S.Z., Bass, I.A., Yurieva, O.V., Minakhina, S.V., Nikiforov, V.G., 1995. Four genes, two ends, and a res region are involved in transposition of Tn*5053*: a paradigm for a novel family of transposons carrying either a mer operon or an integron. Mol. Microbiol. 17 (6), 1189–1200. https://doi.org/10.1111/j.1365-2958.1995.mmi_17061189.x.

Kumar, S., Stecher, G., Tamura, K., 2016. MEGA7: molecular evolutionary genetics analysis version 7.0 for bigger datasets. Mol. Biol. Evol. 33, 1870–1874. https://doi.org/10.1093/molbev/msw054.

L'Abée-Lund, T.M., Sørum, H., 2000. Functional Tn*5393*-like transposon in the R plasmid pRAS2 from the fish pathogen *Aeromonas salmonicida* subspecies *salmonicida* isolated in Norway. Appl. Environ. Microbiol. 66 (12), 5533–5535. https://doi.org/10.1128/aem.66.12.5533-5535.2000.

Lee, K., Lim, J.B., Yum, J.H., Yong, D., Chong, Y., Kim, J.M., Livermore, D.M., 2002. bla_{VIM-2} cassette-containing novel integrons in metallo-β-lactamase-producing *Pseudomonas aeruginosa* and *Pseudomonas putida* isolates disseminated in a Korean hospital. Antimicrob. Agents Chemother. 46, 1053–1058. https://doi.org/10.1128/AAC.46.4.1053-1058.2002.

Limansky, A., Viale, A., 2002. Can composition and structural features of oligonucleotides contribute to their wide-scale applicability as random PCR primers in mapping bacterial genome diversity? J. Microbiol. Methods 50, 291–297. https://doi.org/10.1016/s0167-7012(02)00040-4.

Loucif, L., Cherak, Z., Chamlal, N., Bendjama, E., Gacemi-Kirane, D., Grainat, N., Rolain, J.M., 2017. First detection of VIM-2 Metallo-β-lactamase-producing *Pseudomonas putida* in *Blattella germanica* cockroaches in an Algerian Hospital. Antimicrob. Agents Chemother. 61 (8) https://doi.org/10.1128/AAC.00357-17 e00357–17.

Marchiaro, P., Mussi, M.A., Ballerini, V., Pasteran, F., Viale, A.M., Vila, A.J., Limansky, A.S., 2005. Sensitive EDTA-based microbiological assays for the detection of metallo-β-lactamases in non-fermentative gram-negative bacteria. J. Clin. Microbiol. 43, 5648–5652. https://doi.org/10.1128/jcm.43.11.5648-5652.2005.

Marchiaro, P., Viale, A.M., Ballerini, V., Rossignol, G., Vila, A.J., Limansky, A., 2010. First report of a Tn*402*-like class 1 integron carrying bla_{VIM-2} in *Pseudomonas putida* from Argentina. J. Infect. Dev. Ctries 4, 412–416. https://doi.org/10.3855/jidc.1012.

Marchiaro, P., Brambilla, L., Morán-Barrio, J., Revale, S., Pasteran, F., Vila, A.J., Viale, A. M., Limansky, A., 2014. The complete nucleotide sequence of the carbapenem resistance-conferring conjugative plasmid pLD209 from a *Pseudomonas putida* clinical strain revealed a chimeric design formed by modules derived from both environmental and clinical bacteria. Antimicrob. Agents Chemother. 58, 1816–1821. https://doi.org/10.1128/AAC.02494-13.

Minakhina, S., Kholodii, G., Mindlin, S., Yurieva, O., Nikiforov, V., 1999. Tn*5053* family transposons are *res* site hunters sensing plasmidal *res* sites occupied by cognate resolvases. Mol. Microbiol. 33, 1059–1068. https://doi.org/10.1046/j.1365-2958.1999.01548.x.

Molina, L., Bernal, P., Udaondo, Z., Segura, A., Ramos, J.L., 2013. Complete genome sequence of a *Pseudomonas putida* clinical isolate, strain H8234. Genome Announc 1 (4). https://doi.org/10.1128/genomeA.00496-13 e00496–13.

Mulet, M., Lalucat, J., García-Valdés, E., 2010. DNA sequence-based analysis of the *Pseudomonas* species. Environ. Microbiol. 12, 1513–1530. https://doi.org/10.1111/j.1462-2920.2010.02181.x.

Molina-Mora, J.A., Chinchilla-Montero, D., García-Batán, R., García, F., 2021. Genomic context of the two integrons of ST-111 *Pseudomonas aeruginosa* AG1: a VIM-2-carrying old-acquaintance and a novel IMP-18-carrying integron. Infect. Genet. Evol. 89, 104740. https://doi.org/10.1016/j.meegid.2021.104740.

Mulet, M., García-Valdés, E., Lalucat, J., 2013. Phylogenetic affiliation of *Pseudomonas putida* biovar a and B strains. Res. Microbiol. 164, 351–359. https://doi.org/10.1016/j.resmic.2013.01.009.

Nicolas, E., Lambin, M., Dandoy, D., Galloy, C., Nguyen, N., Oger, C.A., Hallet, B., 2015. The Tn*3*-family of replicative transposons. Microbiol Spectr 3. https://doi.org/10.1128/microbiolspec.MDNA3-0060-2014. MDNA3-0060-2014.

Ochman, H., Gerber, A.S., Hartl, D.L., 1988. Genetic applications of an inverse polymerase chain reaction. Genetics 120 (3), 621–623. https://doi.org/10.1093/genetics/120.3.621.

Papagiannitsis, C.C., Tzouvelekis, L.S., Miriagou, V., 2009. Relative strengths of the class 1 integron promoter hybrid 2 and the combinations of strong and hybrid 1 with an active p2 promoter. Antimicrob. Agents Chemother. 53, 277–280. https://doi.org/10.1128/AAC.00912-08.

Papagiannitsis, C.C., Medvecky, M., Chudejova, K., Skalova, A., Rotova, V., Spanelova, P., Jakubu, V., Zemlickova, H., Hrabak, J., Czech Participants of the European Antimicrobial Resistance Surveillance Network, 2017. Molecular characterization of carbapenemase-producing *Pseudomonas aeruginosa* of Czech origin and evidence for clonal spread of extensively resistant sequence type 357 expressing IMP-7 metallo-β-lactamase. Antimicrob. Agents Chemother. 61 https://doi.org/10.1128/AAC.01811-17 e01811–17.

Papagiannitsis, C.C., Verra, A., Galani, V., Xitsas, S., Bitar, I., Hrabak, J., Petinaki, E., 2020. Unravelling the features of success of VIM-producing ST111 and ST235 *Pseudomonas aeruginosa* in a Greek hospital. Microorganisms. 8 (12), 1884. https://doi.org/10.3390/microorganisms8121884.

Partridge, S.R., Recchia, G.D., Stokes, H.W., Hall, R.M., 2001. Family of class 1 integrons related to In*4* from Tn*1696*. Antimicrob. Agents Chemother. 45 (11), 3014–3020. https://doi.org/10.1128/AAC.45.11.3014-3020.2001.

Partridge, S.R., Kwong, S.M., Firth, N., Jensen, S.O., 2018. Mobile genetic elements associated with antimicrobial resistance. Clin. Microbiol. Rev. 31 https://doi.org/10.1128/CMR.00088-17 e00088–17.

Peix, A., Ramírez-Bahena, M.H., Velázquez, E., 2018. The current status on the taxonomy of *Pseudomonas* revisited: an update. Infect. Genet. Evol. 57, 106–116. https://doi.org/10.1016/j.meegid.2017.10.026.

Perez, F., Hujer, A.M., Marshall, S.H., et al., 2014. Extensively drug-resistant *Pseudomonas aeruginosa* isolates containing bla_{VIM-2} and elements of *Salmonella* Genomic Island 2: a new genetic resistance determinant in Northeast Ohio. Antimicrob. Agents Chemother. 58 (10), 5929–5935. https://doi.org/10.1128/AAC.02372-14.

Peter, S., Oberhettinger, P., Schuele, L., Dinkelacker, A., Vogel, W., Dörfel, D., Bezdan, D., et al., 2017. Genomic characterization of clinical and environmental *Pseudomonas putida* group strains and determination of their role in the transfer of antimicrobial resistance genes to *Pseudomonas aeruginosa*. BMC Genomics 18 (1), 859. https://doi.org/10.1186/s12864-017-4216-2.

Petrovski, S., Stanisich, V.A., 2010. Tn*502* and Tn*512* are *res* site hunters that provide evidence of resolvase-independent transposition to random sites. J. Bacteriol. 192, 1865–1874. https://doi.org/10.1128/JB.01322-09.

Quinones-Falconi, F., Galicia-Velasco, M., Marchiaro, P., Mussi, M.A., Ballerini, V., Vila, A.J., Viale, A.M., Bermejo-Morales, K., Limansky, A.S., 2010. Emergence of *Pseudomonas aeruginosa* strains producing metallo-β-lactamases of the IMP-15 and VIM-2 types in Mexico. Clin. Microbiol. Infect. 16, 126–131. https://doi.org/10.1111/j.1469-0691.2009.02780.x.

Rådström, P., Sköld, O., Swedberg, G., Flensburg, J., Roy, P.H., Sundström, L., 1994. Transposon Tn*5090* of plasmid R751, which carries an integron, is related to Tn7, Mu, and the retroelements. J. Bacteriol. 176 (11), 3257–3268. https://doi.org/10.1128/jb.176.11.3257-3268.1994.

Rogowsky, P., Halford, S.E., Schmitt, R., 1985. Definition of three resolvase binding sites at the *res* loci of Tn*21* and Tn*1721*. EMBO J. 4 (8), 2135–2141.

Sambrok, J., Fritsch, E.F., Maniatis, T., 1989. Molecular Cloning. A Laboratory Manual. Cold Spring Harbor Laboratory Press, Cold Spring Harbor, NY.

Santos, C., Caetano, T., Ferreira, S., Mendo, S., 2010. Tn*5090*-like class 1 integron carrying bla_{VIM-2} in a *Pseudomonas putida* strain from Portugal. Clin. Microbiol. Infect. 16, 1558–1561. https://doi.org/10.1111/j.1469-0691.2010.03165.x.

Scotta, C., Juan, C., Cabot, G., Oliver, A., Lalucat, J., Bennasar, A., Alberti, S., 2011. Environmental microbiota represents a natural reservoir for dissemination of clinically relevant metallo-β-lactamases. Antimicrob. Agents Chemother. 54, 5376–5379. https://doi.org/10.1128/AAC.00716-11.

Seok, Y., Shin, H., Lee, Y., Cho, I., Na, S., et al., 2010. First report of bloodstream infection caused by *Pseudomonas fulva*. J. Clin. Microbiol. 48, 2656–2657. https://doi.org/10.1128/JCM.01609-09.

Shapiro, J.A., Sporn, P., 1977. Tn*402*: a new transposable element determining trimethoprim resistance that inserts in bacteriophage lambda. J. Bacteriol. 129, 1632–1635.

Siguier, P., Perochon, J., Lestrade, L., Mahillon, J., Chandler, M., 2006. ISfinder: the reference Centre for bacterial insertion sequences. Nucleic Acids Res. 34, D32–D36. https://doi.org/10.1093/nar/gkj014.

Stokes, H.W., Elbourne, L.D., Hall, R.M., 2007. Tn*1403*, a multiple-antibiotic resistance transposon made up of three distinct transposons. Antimicrob. Agents Chemother. 51 (5), 1827–1829. https://doi.org/10.1128/AAC.01279-06.

Suenaga, H., Yamazoe, A., Hosoyama, A., Kimura, N., Hirose, J., Watanabe, T., Fujihara, H., Futagami, T., Goto, M., Furukawa, K., 2017. Complete genome sequence of the polychlorinated biphenyl-degrading bacterium *Pseudomonas putida* KF715 (NBRC 110667) isolated from biphenyl-contaminated soil. Genome Announc 5. https://doi.org/10.1128/genomeA.01624-16 e01624–16.

Tansirichaiya, S., Rahman, A., Roberts, A.P., 2019. The transposon registry. Mob. DNA 10, 40. https://doi.org/10.1186/s13100-019-0182-3.

Tato, M., Coque, T.M., Baquero, F., Cantón, R., 2010. Dispersal of Carbapenemase bla_{VIM-1} gene associated with different Tn*402* variants, mercury transposons, and conjugative plasmids in *Enterobacteriaceae* and *Pseudomonas aeruginosa*. Antimicrob. Agents Chemother. 54 (1), 320–327. https://doi.org/10.1128/AAC.00783-09.

Taylor, B.L., Zhulin, I.B., 1999. PAS domains: internal sensors of oxygen, redox potential, and light. Microbiol. Mol. Biol. Rev. 63 (2), 479–506. https://doi.org/10.1128/MMBR.63.2.479-506.1999.

Tohya, M., Watanabe, S., Teramoto, K., Uechi, K., Tada, T., Kuwahara-Arai, K., et al., 2019a. *Pseudomonas asiatica* sp. nov., isolated from hospitalized patients in Japan and Myanmar. Int. J. Syst. Evol. Microbiol. 69, 1361–1368. https://doi.org/10.1099/ijsem.0.003316.

Tohya, M., Watanabe, S., Teramoto, K., Shimojima, M., Tada, T., Kuwahara-Arai, K., et al., 2019b. *Pseudomonas juntendi* sp. nov., isolated from patients in Japan and Myanmar. Int. J. Syst. Evol. Microbiol. 69, 3377–3384. https://doi.org/10.1099/ijsem.0.003623.

Treviño, M., Moldes, L., Hernández, M., Martínez-Lamas, L., García-Riestra, C., Regueiro, B.J., 2010. Nosocomial infection by VIM-2 metallo-beta-lactamase-producing *Pseudomonas putida*. J. Med. Microbiol. 59 (7), 853–855. https://doi.org/10.1099/jmm.0.018036-0.

Van der Zee, A., Kraak, W.B., Burggraaf, A., Goessens, W.H.F., Pirovano, W., Ossewaarde, J.M., Tommassen, J., 2018. Spread of carbapenem resistance by transposition and conjugation among *Pseudomonas aeruginosa*. Front. Microbiol. 9, 2057. https://doi.org/10.3389/fmicb.2018.02057.

Vilacoba, E., Quiroga, C., Pistorio, M., Famiglietti, A., Rodríguez, H., Kovensky, J., Centrón, D., 2014. A bla_{VIM-2} plasmid disseminating in extensively drug-resistant clinical *Pseudomonas aeruginosa* and *Serratia marcescens* isolates. Antimicrob. Agents Chemother. 58, 7017–7018. https://doi.org/10.1128/AAC.02934-14.

Walsh, T.R., Toleman, M.A., Poirel, L., Nordmann, P., 2005. Metallo-beta-lactamases: the quiet before the storm? Clin. Microbiol. Rev. 18 (2), 306–325. https://doi.org/10.1128/CMR.18.2.306-325.2005.

Yamamoto, M., Matsumura, Y., Gomi, R., Matsuda, T., Nakano, S., Nagao, M., Tanaka, M., Ichiyama, S., 2018. Molecular analysis of bla_{IMP-1}-harboring class 3 integron in multidrug-resistant *Pseudomonas fulva*. Antimicrob. Agents Chemother. 62 (8) https://doi.org/10.1128/AAC.00701-18 e00701–18.

Yoon, E.J., Jeong, S.H., 2021. Mobile Carbapenemase Genes in *Pseudomonas aeruginosa*. Front. Microbiol. 12, 614058. https://doi.org/10.3389/fmicb.2021.614058.

Zankari, E., Hasman, H., Cosentino, S., Vestergaard, M., Rasmussen, S., Lund, O., Aarestrup, F.M., Larsen, M.V., 2012. Identification of acquired antimicrobial resistance genes. J. Antimicrob. Chemother. 67 (11), 2640–2644. https://doi.org/10.1093/jac/dks261.